Progress In Electromagnetics Research Letters, Vol. 105, 1–8, 2022

A Novel DGS-Based Substrate Integrated Coaxial Line Bandpass Filter with Three Transmission Zeros

Zhongbao Wang*, Jian Ma, Shipeng Zhao, Hongmei Liu, and Shaojun Fang

Abstract—A novel high-selectivity bandpass filter based on a defected ground structure and substrate integrated coaxial line is proposed. Three transmission zeros near the passband are achieved by introducing a divergent-shaped resonator and two spindle-shaped defected ground structures, resulting in a high selectivity. To verify the proposed structure, one prototype with a center frequency of 4.94 GHz is designed and fabricated. The measured results show that three transmission zeros respectively located at 3.92, 4.36, and 6.00 GHz are obtained. The 3-dB passband bandwidth is 14.2% from 4.59 to 5.29 GHz. The upper stopband rejection is better than 20 dB from 5.71 to 11.31 GHz.

1. INTRODUCTION

Bandpass filter with high selectivity and good stopband rejection plays an important role in microwave circuits and systems. As a general transmission line commonly used in microwave and millimeter systems, a substrate integrated coaxial line (SICL) was proposed in [1]. SICL exhibits the same characteristics as traditional coaxial lines. They are both shielded and non-dispersive TEM-guided wave structures. This means that SICL also has the advantages of high Q value, low loss, small size, and low cost, and can be realized by a simple and cheap printed circuit board (PCB) process. Recently, several SICL bandpass filters have been presented. In [2] and [3], quarter-wavelength stepped-impedance and spiral resonators based on SICL were used to reduce the filter size. In [4] and [5], open stubs were adopted in stepped-impedance SICL resonators to design wide stopband SICL bandpass filters. However, the insertion losses of these designs are larger than 2 dB, and the selectivity [3–5] needs to be enhanced.

Usually, the method of adding transmission zeros (TZs) is used to improve the selectivity of the bandpass filter. In [6], a filtering building block consisting of a dual-mode substrate integrated waveguide (SIW) coaxial cavity was proposed to generate one TZ, which can be placed either below or above the passband. In [7], an SICL non-resonating node (NRN) was inserted in the SIW filter to generate two TZs, which are respectively located at the two sides of the passband. However, the locations of the two TZs cannot be changed flexibly. In [8], an asymmetrical spiral stub-loaded SICL resonator was proposed to obtain multiple TZs. However, the TZs are far from the passband.

In addition, defected ground structure (DGS) can provide a band-rejection characteristic [9], which can be used to improve the filtering performance. In [10], a cross slot DGS was adopted in SIW filters to improve their upper stopband rejection property. In [11], H- and U-shaped DGSs were added to a coupled microstrip filter to increase the bandwidth of the passband. In [12], a Koch fractal DGS was used to improve the stopband performance of a low-pass filter. In [13], the common-mode suppression of an ultra-wideband differential bandpass filter was improved by a DGS. In [14], a super-wide-band SIW filter was realized by using a DGS. To the best of our knowledge, DGS-based SICL filter has not been reported before.

Received 8 May 2022, Accepted 6 June 2022, Scheduled 21 June 2022
* Corresponding author: Zhongbao Wang (wangzb@dlmu.edu.cn).
The authors are with the School of Information Science and Technology, Dalian Maritime University, Dalian 116026, Liaoning, China.

In this paper, a novel high-selectivity DGS-based SICL bandpass filter is proposed. Three TZs near the passband are achieved by introducing a divergent-shaped resonator and two spindle-shaped DGSs. Square ring slot DGSs are used to tune the position of two TZs below the passband and the bandwidth of the passband. Besides, the proposed filter has low insertion loss.

2. FILTER DESIGN AND PARAMETRIC STUDIES

The proposed DGS-based SICL bandpass filter is illustrated in Fig. 1. The whole structure is compatible with the standard PCB process. The upper and lower substrates are tightly attached through metal shorting pins. The two substrates have the same thickness $H = 1.0\,\text{mm}$, dielectric constant $\varepsilon_r = 2.73$, and loss tangent $\tan\delta = 0.003$. The top copper cladding is shown in Fig. 1(b). The square ring slot DGSs are located at the centre of the upper ground plane to tune the filtering performances. The number of square ring slots is $N = 3$.

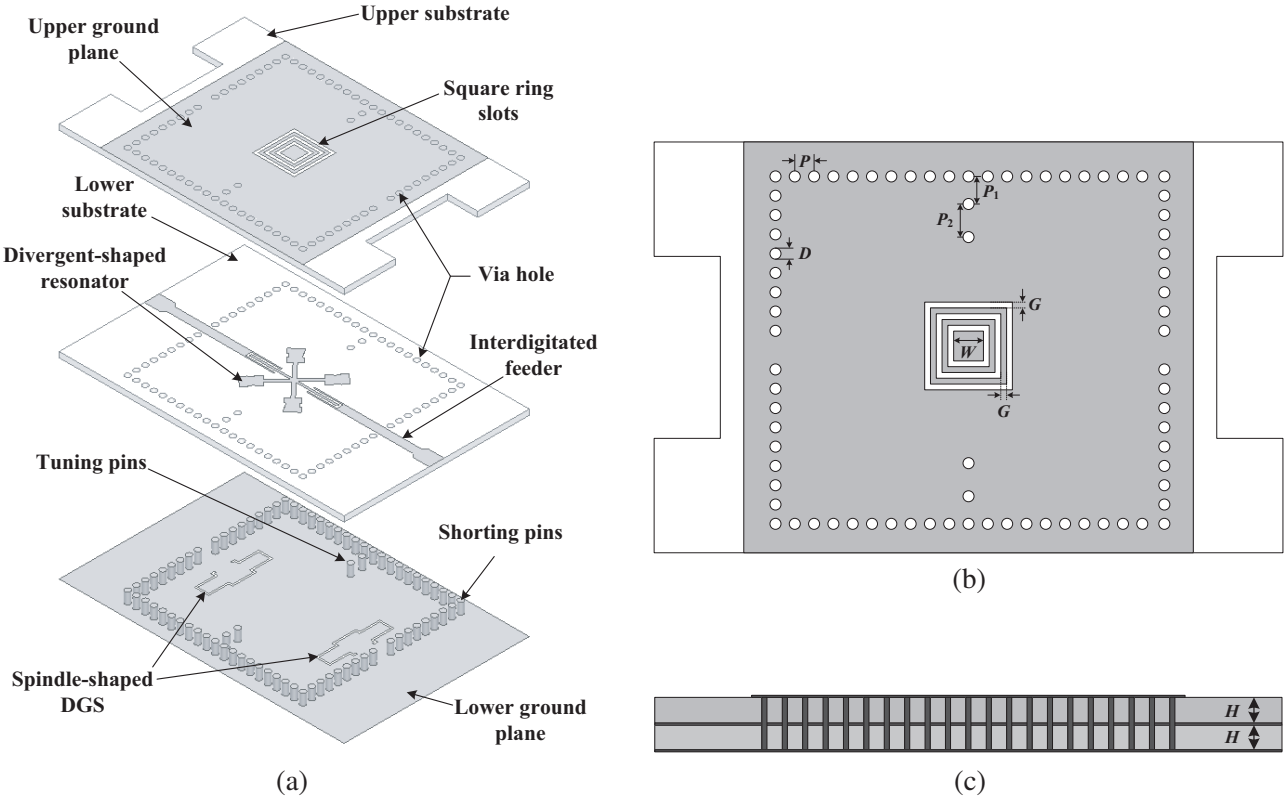

Figure 1. Configuration of the proposed DGS-based SICL bandpass filter. (a) Exploded view. (b) Top view. (c) Side view. ($D = 1.0\,\text{mm}$, $P = 1.6\,\text{mm}$, $P_1 = 2.0\,\text{mm}$, $P_2 = 2.1\,\text{mm}$, $G = 0.25\,\text{mm}$, $W = 2.5\,\text{mm}$).

The middle copper cladding and the lower ground plane with DGSs are shown in Fig. 2. The middle copper cladding is arranged on the upper surface of the lower substrate, which contains a divergent-shaped resonator and two interdigitated feeders. The divergent-shaped resonator is composed of four identical quarter-wavelength stepped-impedance lines and two quarter-wavelength high-impedance lines. The main mode of the divergent-shaped resonator and the shielded cavity both resonate at the center frequency of the bandpass filter. Four tuning pins in the shielded cavity are used to tune its resonant frequency for impedance matching in the passband. In Fig. 2(b), two spindle-shaped DGSs are symmetrically arranged in the lower ground plane.

The design of the proposed DGS-based SICL bandpass filter is based on the evolution steps that

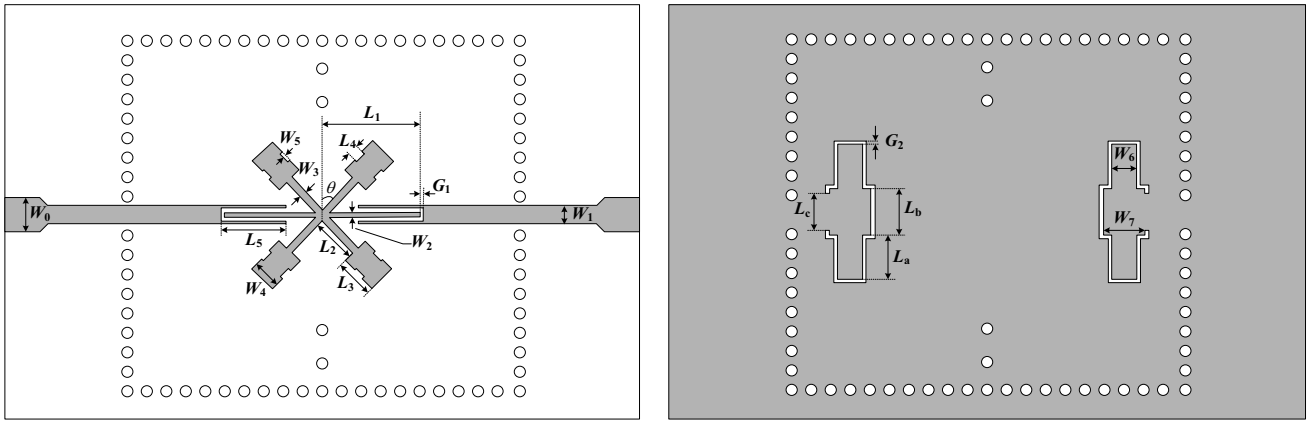

(a) (b)

Figure 2. (a) Middle copper cladding and (b) lower ground plane with DGS ($W_0 = 2.75\,\text{mm}$, $W_1 = 1.5\,\text{mm}$, $W_2 = 0.75\,\text{mm}$, $W_3 = 0.6\,\text{mm}$, $W_4 = 2.3\,\text{mm}$, $W_5 = 0.2\,\text{mm}$, $W_6 = 2\,\text{mm}$, $W_7 = 3.4\,\text{mm}$, $L_1 = 8.0\,\text{mm}$, $L_2 = 3.95\,\text{mm}$, $L_3 = 3.2\,\text{mm}$, $L_4 = 0.9\,\text{mm}$, $L_5 = 5.0\,\text{mm}$, $L_a = 3.6\,\text{mm}$, $L_b = 3.8\,\text{mm}$, $L_c = 3\,\text{mm}$, $G_1 = 0.35\,\text{mm}$, $G_2 = 0.3\,\text{mm}$, $\theta = 43\,\text{deg}$).

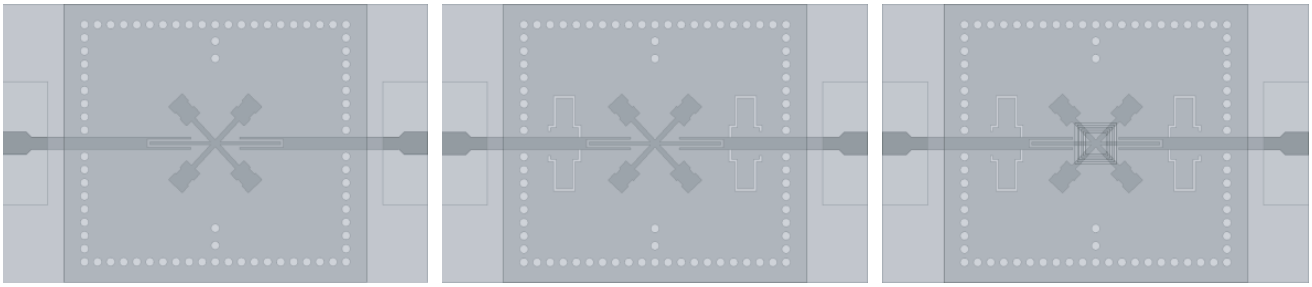

(a) (b) (c)

Figure 3. Design evolution of the proposed DGS-based SICL bandpass filter. (a) Step-1. (b) Step-2. (c) Step-3.

are illustrated in Fig. 3 along with its corresponding simulated S-parameters in Fig. 4. The evolution procedure is as follows:

1) In Step-1, the lengths of the $\lambda/4$ stepped-impedance lines and the $\lambda/4$ high-impedance lines for the divergent-shaped resonator are determined by choosing the appropriate widths according to the center frequency of the bandpass filter, and the dimension of the shielded cavity is chosen about $0.85\lambda \times 0.78\lambda$.

2) Two spindle-shaped DGSs are added to the filter in Step-2. The slot length of the spindle-shaped DGS is about $\lambda/2$. TZs are obtained, and a second-order filter is formed.

3) In Step-3, three square ring slots are etched in the upper ground plane to tune the filtering performances, and the size of the square ring slots is determined according to the required 3-dB passband bandwidth.

Figure 5 shows the simulation results of the proposed DGS-based SICL bandpass filter. There are three TZs named as TZ_1, TZ_2, and TZ_3. The spindle-shaped DGS controls one TZ which is TZ_1, and the divergent-shaped resonator controls two TZs which are TZ_2 and TZ_3. Fig. 6 gives the effect of the size (L_a) of the spindle-shaped DGS on $|S_{21}|$ of the proposed DGS-based SICL bandpass filter. It can be found that when the length L_a is decreased from 3.72 to 3.48 mm (i.e., the slot length of the spindle-shaped DGS is decreased), the TZ_1 moves towards the passband; the stopband rejection between the TZ_1 and TZ_2 becomes better; and the position of TZ_3 almost is unchanged. This indicates

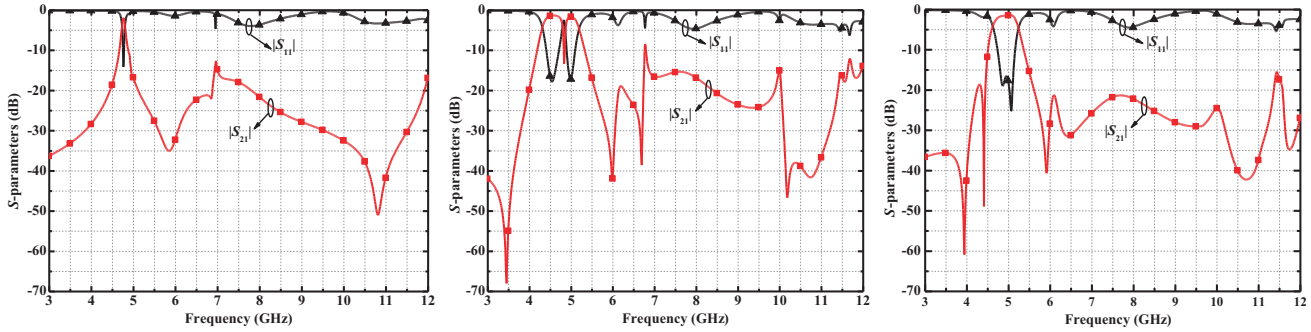

Figure 4. Simulated S-parameters of the SICL filter structures corresponding to (a) Step-1, (b) Step-2, and (c) Step-3.

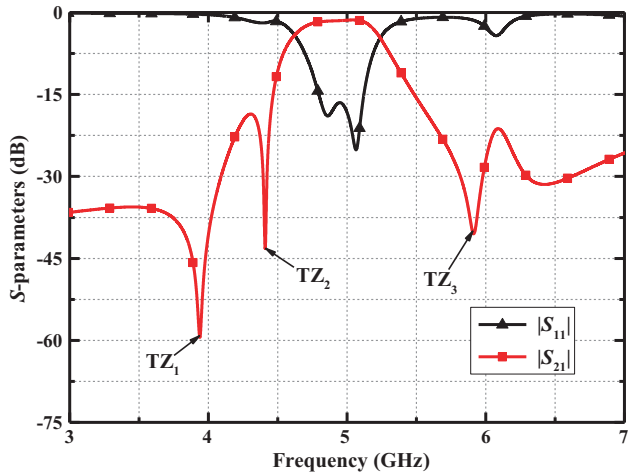

Figure 5. Simulated S-parameters of the proposed DGS-based SICL bandpass filter.

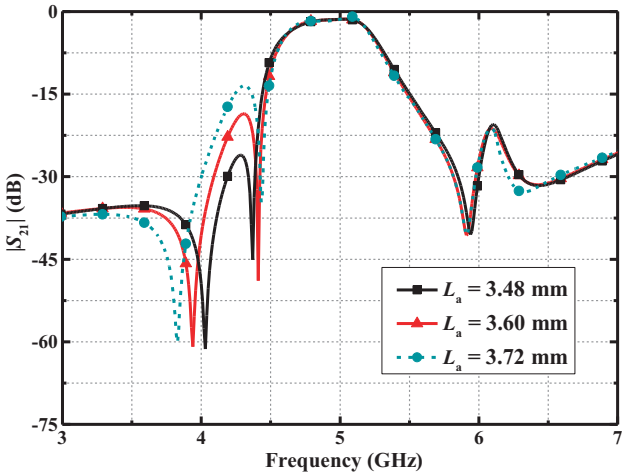

Figure 6. Effect of the L_a on the $|S_{21}|$ of the proposed DGS-based SICL bandpass filter.

that TZ_1 is controlled by the spindle-shaped DGS.

Figure 7 shows the effect of the sizes (L_1 and L_2) of the divergent-shaped resonator on $|S_{21}|$ of the proposed filter. It can be seen from Fig. 7(a) that when L_1 is decreased from 8.3 to 7.7 mm (i.e., the length of the high-impedance line is decreased), the TZ_3 shifts towards the passband. Under the condition that the total length ($L_2 + L_3 = 7.15$ mm) remains unchanged, the influence of L_2 on the $|S_{21}|$ is shown in Fig. 7(b). When L_2 is reduced from 4.4 to 3.5 mm (i.e., the length proportion of the stepped-impedance line is changed), the TZ_2 shifts to a lower frequency; the stopband rejection between the TZ_1 and TZ_2 becomes better; and the 3-dB passband bandwidth becomes wider. Fig. 7 indicates that TZ_2 and TZ_3 are controlled by the divergent-shaped resonator.

Figure 8 gives the effect of the square ring slot DGS on the $|S_{21}|$ of the proposed filter. When the number N of square ring slots is larger than 3, TZ_1 and TZ_2 will disappear, but the upper stopband suppression will become better. Thus, the number N of square ring slots is selected as 3 to retain the TZs and obtain better upper stopband suppression. When W is increased from 2.3 to 2.7 mm, TZ_1 and TZ_2 will be merged together with a deteriorated selectivity and an expanded 3-dB passband bandwidth. Therefore, there is a compromise between the selectivity and passband bandwidth.

Figure 9 shows the effect of the distance P_1 of tuning pins on the $|S_{11}|$ of the proposed filter. When P_1 is decreased from 2.3 to 1.7 mm, the two resonant frequencies of the filter move towards the center frequency, and $|S_{11}|$ in the passband will become better. This indicates that the tuning pins can be used to realize the impedance matching in the passband.

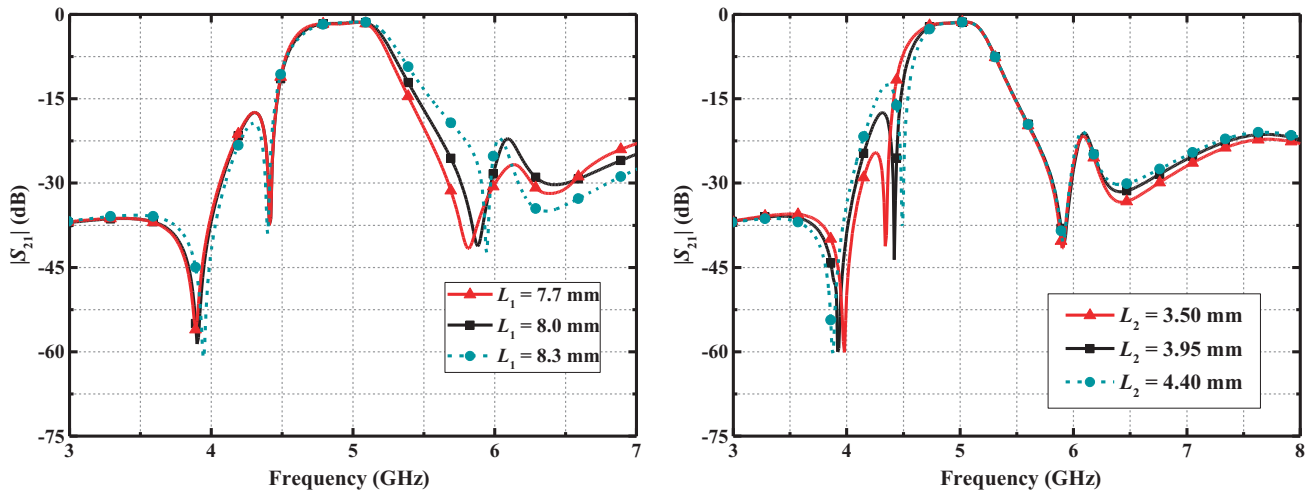

Figure 7. Effect of the L_1 and L_2 on the $|S_{21}|$ of the proposed DGS-based SICL bandpass filter. (a) L_1. (b) L_2.

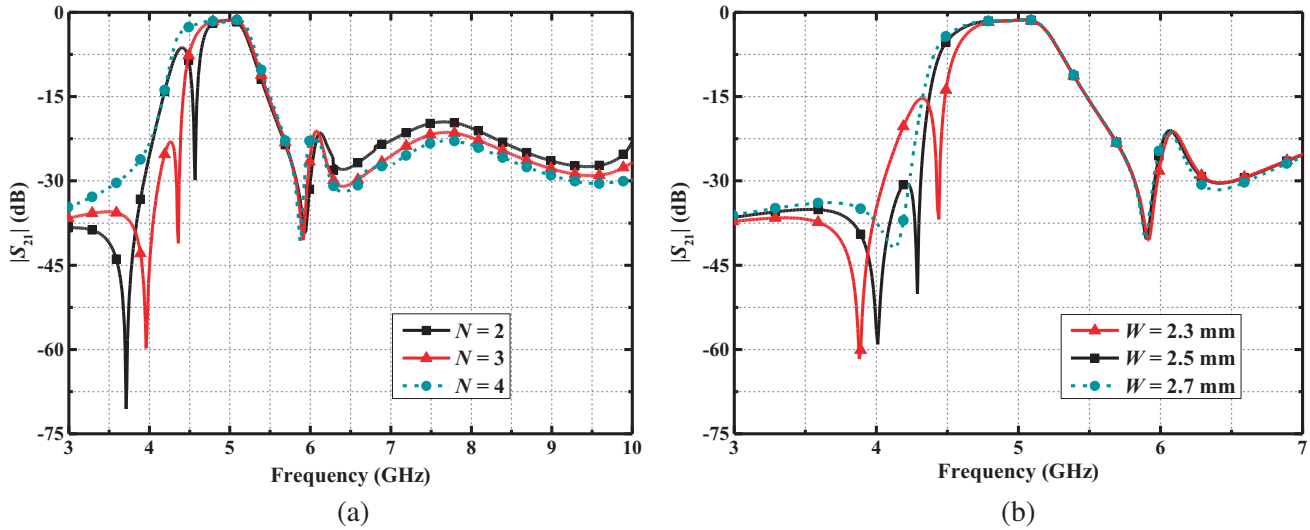

Figure 8. Effect of the square ring slot DGS on the $|S_{21}|$ of the proposed DGS-based SICL bandpass filter. (a) The number N of square ring slots. (b) W.

3. IMPLEMENTATION AND PERFORMANCE

The prototype of the proposed DGS-based SICL bandpass filter is fabricated and shown in Fig. 10. The S-parameters are measured by an Agilent N5230A vector network analyzer.

Figure 11 gives the simulated and measured S-parameters of the proposed DGS-based SICL bandpass filter. Good agreements are obtained between simulation and measurement results. The measured insertion loss is 1.55 dB at the center frequency f_0 of 4.94 GHz. The measured 3-dB fractional bandwidth (FBW) is 14.2% from 4.59 to 5.29 GHz. The upper stopband rejection is better than 20 dB from 5.71 to 11.31 GHz. Three transmission zeros respectively located at 3.92, 4.36, and 6.00 GHz are obtained. Table 1 shows the comparison of the proposed DGS-based SICL bandpass filter with previous designs. Compared with [2–8], the proposed DGS-based SICL bandpass filter has more TZs near the passband, lower insertion loss, and wider 3-dB bandwidth.

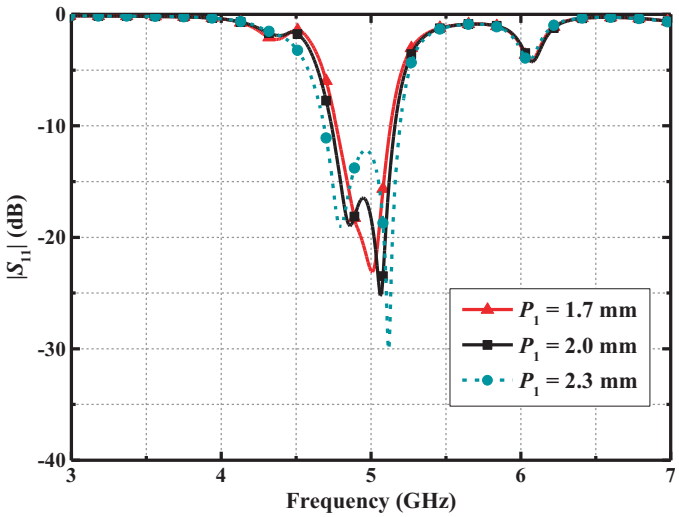

Figure 9. Effect of the tuning pins on the $|S_{11}|$ of the proposed DGS-based SICL bandpass filter.

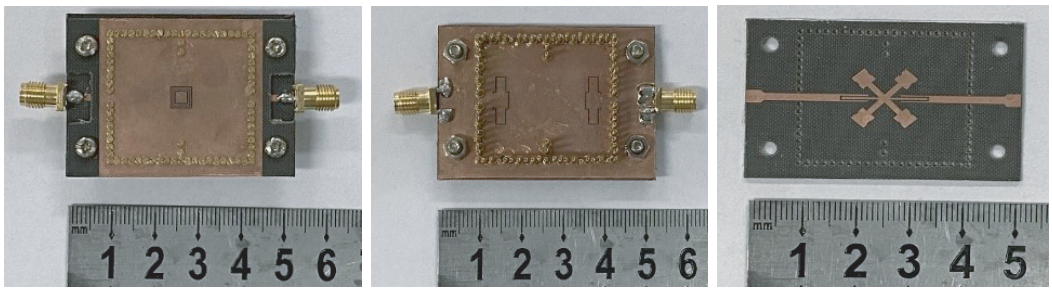

(a) (b) (c)

Figure 10. Photographs of the fabricated DGS-based SICL bandpass filter. (a) Top view. (b) Bottom view. (c) Intermediate structure.

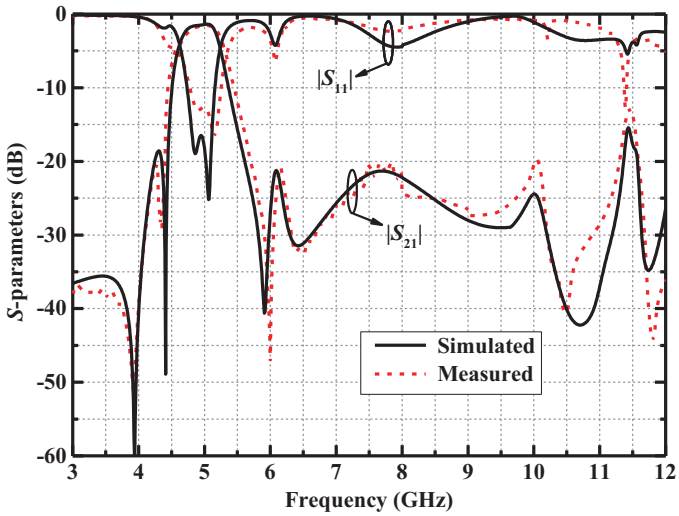

Figure 11. Simulated and measured S-parameters of the proposed DGS-based SICL bandpass filter.

Table 1. Performance comparison.

References	Type	f_0 (GHz)	FBW (%)	IL (dB)	TZs*	Size# ($\lambda_0 \times \lambda_0$)
[2]	SICL	2.39	10	2.4	2	0.168×0.088
[3]	SICL	1.18	7.5	2.7	0	0.047×0.047
[4]	SICL	2.40	5.0	2.4	0	0.132×0.081
[5]	SICL	2.39	3.8	3.0	0	0.129×0.081
[6]	SIW-DGS	8	5.0	1.7	1	0.22×0.22
[7]	SIW-NRN	28	3.6	2.2	2	1.53×0.53
[8]	SICL	1.04	4.8	1.65	2	0.051×0.044
This work	SICL-DGS	4.94	14.2	1.55	3	0.61×0.59

* The number of TZs near the passband. # Circuit size excluding two feeding lines.

4. CONCLUSION

In this paper, a high-selectivity DGS-based SICL bandpass filter has been presented. By introducing a divergent-shaped resonator and two spindle-shaped DGSs, three TZs near the passband have been achieved, which effectively enhances the filter's frequency selectivity. The position of two TZs below the passband and the bandwidth of the passband can be tuned by the square ring slot DGSs. The flexible impedance matching in the passband has been realized by the tuning pins. Compared with the existing SICL bandpass filter, the proposed filter has more TZs near the passband (higher selectivity), lower insertion loss, and wider 3-dB bandwidth. So it can be applied to various wideband microwave communication systems.

ACKNOWLEDGMENT

This work was supported by the National Natural Science Foundation of China (No. 61871417), the LiaoNing Revitalization Talents Program (No. XLYC2007024), the Natural Science Foundation of Liaoning Province (No. 2020-MS-127), and the Fundamental Research Funds for the Central Universities (No. 3132022243).

REFERENCES

1. Gatti, F., M. Bozzi, L. Perregrini, K. Wu, and R. G. Bosisio, "A novel substrate integrated coaxial line (SICL) for wide-band applications," *Eur. Microwave Conf.*, 1614–1617, Manchester, 2006.
2. Chu, P., W. Hong, K. Wu, J. Chen, and H. Tang, "A miniaturized bandpass filter implemented with substrate integrated coaxial line," *Microw. Opt. Techn. Lett.*, Vol. 55, No. 1, 131–133, Jan. 2013.
3. Lu, Y.-L., G.-L. Dai, C. Hua, G. Xu, and K. Li, "Design of miniaturized substrate integrated coaxial line bandpass filters with quarter-wavelength spiral resonator," *Int. J. RF Microwave Comput. Aided Eng.*, Vol. 26, No. 6, 489–495, Jun. 2016.
4. Chu, P., W. Hong, L. Dai, H. Tang, Z. Hao, J. Chen, and K. Wu, "Wide stopband bandpass filter implemented with spur stepped impedance resonator and substrate integrated coaxial line technology," *IEEE Microw. Wireless Compon. Lett.*, Vol. 24, No. 4, 218–220, Apr. 2014.
5. Chu, P., L. Guo, L. Zhang, and K. Wu, "Wide stopband bandpass filter implemented by stepped impedance resonator and multiple in-resonator open stubs," *IEEE Access*, Vol. 7, 140631–140636, Sept. 2019.
6. Sanchez-Soriano, M. A., S. Sirci, J. D. Martinez, and V. E. Boria, "Compact dual-mode substrate integrated waveguide coaxial cavity for bandpass filter design," *IEEE Microw. Wireless Compon. Lett.*, Vol. 26, No. 6, 386–388, Jun. 2016.

7. He, Z., C. J. You, S. Leng, and X. Li, "Compact inline substrate integrated waveguide filter with enhanced selectivity using new non-resonating node," *Electron. Lett.*, Vol. 52, No. 21, 1778–1780, Oct. 2016.
8. Lu, Y., Y. Wang, T. Liu, B. Yu, and K. Li, "Miniaturized substrate-integrated coaxial line bandpass filter with improved upper stopband," *Int. J. Microw. Wirel. Technol.*, Vol. 9, No. 7, 1441–1445, Sept. 2017.
9. Woo, D.-J., T.-K. Lee, J.-W. Lee, C.-S. Pyo, and W.-K. Choi, "Novel U-slot and V-slot DGSs for bandstop filter with improved Q factor," *IEEE Trans. Microw. Theory Techn.*, Vol. 54, No. 6, 2840–2847, Jun. 2006.
10. Zhang, Y. L., W. Hong, K. Wu, J. X. Chen, and H. J. Tang, "Novel substrate integrated waveguide cavity filter with defected ground structure," *IEEE Trans. Microw. Theory Techn.*, Vol. 53, No. 4, 1280–1287, Apr. 2005.
11. Azizi, S., M. E. Gharbi, S. Ahyoud, and A. Asselman, "Design of bandpass filter for C application with improved selectivity," *Mediterr. Congr. Telecommun*, 1–4, Fez, Morocco, 2019.
12. Wen, Z.-L., Y.-N Han, X.-Y. Sun, et al., "Design of miniaturized low-pass filter with improved Koch fractal DGS," *IEEE Int. Symp. Electromagn. Compat.*, 1–4, Beijing, China, 2017.
13. Shi, S., W. Choi, W. Che, K. Tam, and Q. Xue, "Ultra-wideband differential bandpass filter with narrow notched band and improved common-mode suppression by DGS," *IEEE Microw. Wireless Compon. Lett.*, Vol. 22, No. 4, 185–187, Apr. 2012.
14. Hao, Z.-C., W. Hong, J.-X. Chen, X.-P. Chen, and K. Wu, "Compact super-wide bandpass substrate integrated waveguide (SIW) filters," *IEEE Trans. Microw. Theory Techn.*, Vol. 53, No. 9, 2968–2977, Sept. 2005.